International Conference on Renewable Energies and Power Quality (ICREPQ'18)
Salamanca (Spain), 21st to 23rd March, 2018
Renewable Energy and Power Quality Journal (RE&PQJ)
ISSN 2172-038 X, No.16 April 2018

Optimal design of the on-board electrical generation system of a jet airliner.

F.J. Asensio[1], J.I. San Martín[1], I. Zamora[2], G. Saldaña[1], and A. Mollinedo[1].

[1] Department of Electrical Engineering
Engineering School of Gipuzkoa (Section of Eibar), University of the Basque Country (UPV/EHU)
Campus of Gipuzkoa, 20600 Eibar (Spain)
Phone number: +0034 943 033064, e-mail: joseignacio.sanmartín@ehu.eus

[2] Department of Electrical Engineering
Engineering School of Bilbao, University of the Basque Country (UPV/EHU)
Campus of Biscay, 48013 Bilbao (Spain)
Phone number: +0034 946 014063, e-mail: inmaculada.zamora@ehu.eus

Abstract. This paper proposes a new design for the on-board electrical generation system of the commercial airplane Boeing 747. In addition to the on-board energy generation, the proposed design also contemplates energy recovery during landing by regenerative braking. The proposed system consists of a micro-grid composed of proton exchange membrane fuel cells (PEMFC), Ion-Lithium based cells and reversible electrical synchronous machines. The key aspect of this design relies on the reduction of the weight of the water needed to bring abroad at the moment of taking off. This is possible because it is assumed that the water obtained as by-product of the electrochemical reactions of the fuel cell will be used for sanitary purposes. A study of the economic viability of the design in function of the hydrogen and jet fuel prices has been carried out. Results from simulations in MATLAB have shown a great potential for energy savings and reduction of pollutant emissions.

Key words

Proton Exchange Membrane Fuel Cell (PEMFC); Energy recovery; Regenerative braking; On-board generation, Lithium-ion cell.

1. Introduction

Population growth has led to an increased need for transportation and therefore a greater consumption of energy and fuels, which supposes a greater consumption of resources and an increase of emissions to the atmosphere. World energy consumption increased by 1% in the last three years [1]. In 2015, transport sector accounted for 33.1% of total energy consumption in EU 28, [2]. Nowadays, the transport sector depends on oil and its derivatives by more than 95%, which means that it is very dependent on this type of fuels. Looking ahead to 2020, 74% of energy from oil is expected to be destined to the transport sector [3].

Taking above mentioned percentages into account, the importance of reducing the use of fossil fuels and carbon emissions from aviation sector is shown. In this sense, air vehicles produced 2% of global CO_2 emissions in 2012 and an increase to 3% is expected by 2050 [4].

Approximately, there are more than 100,000 daily flights and around 9,000 airports worldwide. Atlanta, Chicago O'Hare or Los Angeles, among others, are the airports with largest transit of passengers, with 610,000 to 930,000 flights per year. All these data lead to think about the large amount of energy that is currently needed during taxiing movement of airliners, before and after each flight, and during landings. In this sense, it takes a lot of energy to reduce the speed of the airliner when landing, which is done mainly by reverse operation of the reactors, aerodynamic braking and mechanical braking. In addition to the kerosene needed to propel and brake an airplane, more kerosene is also required to supply the electrical energy requirement of the aircraft during the flight, which is produced by electrical machines coupled to the reactors of the airliner.

Airliner reactors, located on wings in the case of all large commercial aircrafts, are machines designed to operate optimally at a certain height, air pressure, temperature and speed; of course, these conditions occur only in the air, when the jet airliner is flying at cruising speed. In this context, when the airliner moves on the landing track, it also uses its reactors, (usually at idle speed), and since they are not designed for ground conditions, they operate at very low efficiency during taxiing and braking operation.

In this sense, this paper focuses on the optimal design of a microgrid composed by a proton exchange membrane fuel cell (PEMFC), reversible electrical synchronous machines and ion-lithium based batteries aimed at maximizing energy efficiency of a jet airliner.

2. Description of the proposed system

Figure 1 shows the scheme of the proposed system. Stored hydrogen is fed to a fuel cell to provide electrical energy during taxiing movement and to supply energy to entertainment equipment, lighting and other ancillary devices during flight.

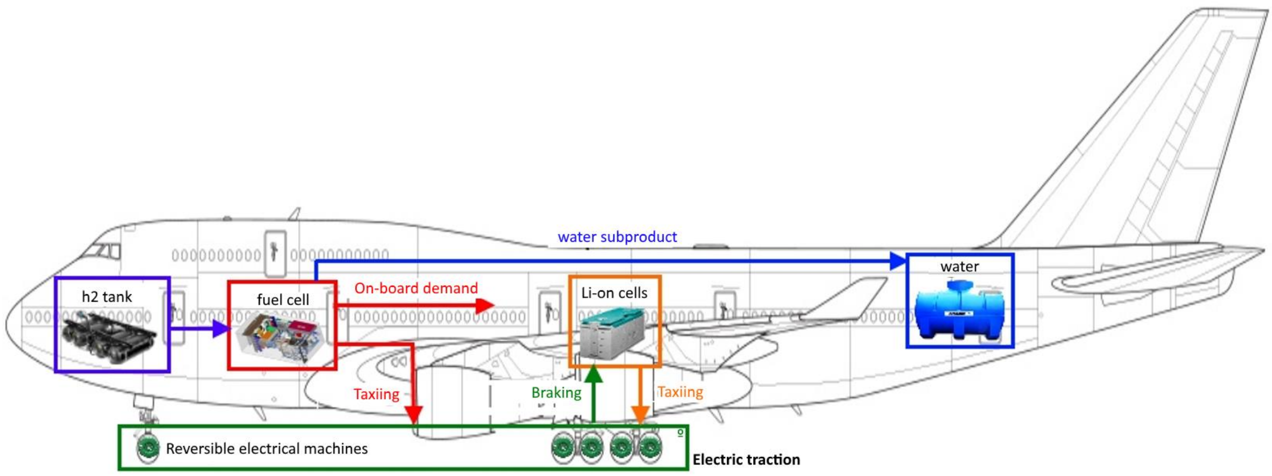

Figure 1. Scheme of the proposed microgrid.

A set of reversible electrical machines are used to provide electric traction during taxiing movement of the airliner and to recover energy when landing. This way, the reversible machines act as motors during taxiing, turning electrical energy into mechanical on the wheels; and later, as generators during braking on landing, turning the mechanical rotation of the wheels into electrical energy, which is stored in li-ion cells. These li-ion cells are used to supply energy to the electrical machines during taxiing movement.

A PEMFC is used to provide the electrical energy necessary during the flight as well as electrical energy to supply the reversible electrical machines during taxiing. The water obtained as by-product of the electrochemical reactions produced in the fuel cell is stored in a water tank. This way, the airliner needs less water during the take-off, which supposes a fuel saving as well as weight saving during take-off.

It is decided to use "In-Wheel" permanent magnet machines housed inside the wheels. The machine used in this proposed optimal design corresponds to a prototype developed by Siemens [5]. These machines have the peculiarity of having an external rotor, which is solidly attached to the inside of the wheel cover, rotating with the wheel. The stator, located in the centre of the machine, is connected to the axle of the wheels, so that it remains static and connects electrically to the corresponding load.

The four most feasible elements to use are batteries, supercapacitors, fuel cells, and flywheels. All these elements could serve in some way in one or more of the three systems to be changed in this project; that is, in traction, energy generation or recovery.

The primary batteries are discarded due to their inability to be charged and to store the energy recovered during braking. Regarding secondary batteries, the most interesting in this case are lithium-ion batteries, mainly because of their specific energy and greater efficiency than the rest, as long as specific controls regarding the operation and possible failures are maintained due to the flammability of the electrolyte [6], [7].

The main advantages of ultracapacitors are the high power density, the low time needed to charge them, the ability to withstand high power peaks, high life cycles and high efficiency. However, they are discarded because of the limited energy density and the working voltage of the banks, approximately set at 500 V maximum [8].

Among the fuel cells, stands out the PEM type in comparison to other types since they are the most promising option for mobile applications and vehicles due to its high electrical efficiency, which is around 50-60%, high current density and power, and its low operating temperature [9-11]. For this case, the fuel cell chosen has been the FCveloCity-HD from Ballard [12].

For the generation of electric power in flight, it is considered an absolute priority to reduce the kerosene consumption and the impact on the environment. In this sense, fuel cells have a great advantage in this aspect since it is possible to use the water generated by the cells on the plane, which allows to reduce a large part of the weight of water usually carried by the plane.

For the taxiing maneuver, however, the lithium batteries are chosen due to their specific power, energy density and long-term savings criteria. In this optimal design, the ABLP9255275HG l-ion cells from Amicell have been used [13].

3. System sizing

In order to guarantee the production of energy on board, it is decided to design a redundant system composed of two fuel cells. Regarding the traction system, this is composed of 18 reversible synchronous machines arranged in the landing gear.

Initially, knowing the energy needs on board, the hydrogen power needed for each fuel cell $P_{hyd,fc}$ has been calculated as shown in equation (1).

$$P_{hyd,fc} = \frac{2 \cdot P_{elect,fc}}{\eta_{fc} \cdot \eta_{cond}} \tag{1}$$

The parameter values of the propulsion system are shown in Table I.

Table I. – Parameter values of the propulsion system [5], [12].

Fuel cell

Parameter	*Value*	*Description*
$P_{nom,fc}$	100 kW	Nominal power
$P_{elect,fc}$	60 kW	Operating point
η_{fc}	0.5	Fuel cell efficiency
η_{cond}	0.95	Power conditioning system efficiency
W_{fc}	410 kg	Fuel cell weight (includes the weight of power conditioning and cooling systems)

Reversible synchronous machine

Parameter	*Value*	*Description*
W_{mot}	50 kg	Weight
$P_{nom,mot}$	260 kW	Nominal power

Assuming an average flight time t_{flight} of 10h, the necessary energy $E_{flight,hyd}$ to be stored in the aircraft is obtained in the equation (2).

$$E_{flight,hyd} = P_{hyd,fc} \cdot t_{flight} \quad (2)$$

By means of the specific weight of hydrogen $E_{spec,hyd}$ from Table II, in equation (3) the necessary energy for the flight is related to the weight of the fuel $W_{flight,hyd}$ to be stored.

$$W_{flight,\mathrm{hyd}} = \frac{\mathrm{E_{flight,hyd}}}{\mathrm{E_{spec,hyd}}} \quad (3)$$

Idem, the weight of the kerosene for the flight $W_{flight,ker}$ has been calculated in equation (4).

$$W_{flight,ker} = \frac{2 \cdot P_{elect,fc} \cdot t_{flight}}{\eta_{turb,flight} \cdot E_{spec,ker}} \quad (4)$$

Table II. – Parameter values of the fuels

Kerosene

Parameter	Value	Description
$E_{spec,ker}$	42.8 MJ/kg	Specific energy

Hydrogen

Parameter	*Value*	*Description*
$Vol_{spec,hyd}$	11.12 Nm^3/kg	Specific volume
$\mathrm{E_{spec,hyd}}$	120 MJ/kg	Specific energy
$F_{compr,1000}$	1.7	Pressure compression factor @ 1000 bar

The weight of the new wheel $W_{tire,new}$ after replacing the tires with engines has been calculated in equation (5), the variation in each tire $W_{tire,eachsav}$ in equation (6) and the net weight variation $W_{tire,sav}$ in equation (7) knowing the number of wheels n_{wheels}. For this, parameters in Table III have been used.

Table III. – Parameter values of the jet airliner [14].

Boeing 747

Parameter	Value	Description
$\eta_{turb,flight}$	0.35	Turbine efficiency
$W_{tire,orig}$	110 kg	Tire weight
W_{tire}	74.4 kg	Rim weight
$W_{max,takeoff}$	362.874 Tn	Max. take-off weight
v_{taxi}	10.29 m/s	Taxiing speed
x_{taxi}	5,000 m	Taxiing distance
t_{taxi}	485.91 s	Taxiing time
v_{land}	72.22 m/s	Landing speed
n_{wheels}	18	Number of wheels

$$W_{tire,new} = W_{tire,orig} - W_{tire} + W_{mot} \quad (5)$$

$$W_{tire,eachsav} = W_{tire,orig} - W_{tire,new} \quad (6)$$

$$W_{tire,sav} = W_{tire,eachsav} \cdot n_{wheels} \quad (7)$$

The energy required in the taxiing movement $E_{c,taxi}$ has been calculated from the kinetic energy expression in equation (8), while the energy necessary to keep the airplane in motion is the energy corresponding to overcome the friction force E_{fric}, as expressed in equation (9).

$$E_{c,taxi} = \frac{1}{2} \cdot W_{max,takeoff} \cdot v_{taxi}^{2} \quad (8)$$

$$E_{fric} = \mu_{rod} \cdot W_{max,takeoff} \cdot g \cdot x_{taxi} \quad (9)$$

Knowing the average time of taxiing, the power to be supplied during this movement $P_{mec,needed}$ has been calculated in equation (10).

$$P_{mec,needed} = \frac{E_{fric}}{t_{taxi}} \quad (10)$$

The mechanical power that the two fuel cells can provide $P_{mec,fc}$ has been calculated in equation (11) considering the efficiency of the fuel cell η_{fc} and the conditioning system η_{cond}. The hydrogen energy $E_{taxi,hyd}$ needed for the taxiing movement during taxiing time t_{taxi} is shown in equation (12).

$$P_{mec,fc} = 2 \cdot P_{nom,fc} \cdot \eta_{fc} \cdot \eta_{cond} \quad (11)$$

$$E_{taxi,hyd} = P_{mec,fc} \cdot t_{taxi} \quad (12)$$

The weight of the hydrogen $W_{taxi,hyd}$ necessary to generate the energy for the taxiing movement has been calculated in equation (13). Besides, the weight of the kerosene $W_{taxi,ker}$ no longer needed for this manoeuvre is shown in equation (14).

$$W_{taxi,hyd} = \frac{E_{taxi,hyd}}{E_{spec,hyd}} \quad (13)$$

$$W_{taxi,ker} = \frac{P_{mec,fc} \cdot t_{taxi}}{\eta_{turb,taxi} \cdot E_{spec,ker}} \quad (14)$$

Since the power required for the taxiing movement is greater than that provided by the fuel cells, the extra power $P_{mec,bat}$ and energy $E_{mec,bat}$ has to be supplied by the batteries, which have been calculated in equation (15) and equation (16) respectively.

$$P_{mec,bat} = P_{mec,needed} - P_{mec,cells} \quad (15)$$

$$E_{mec,bat} = P_{mec,bat} \cdot t_{taxi} \quad (16)$$

The number of battery cells $\boldsymbol{n_{cells}}$ to be installed in series ($\boldsymbol{n_{series}}$) and parallel ($\boldsymbol{n_{paral}}$) as well as the branch voltage $\boldsymbol{V_{branch}}$ and the battery and branch discharge currents ($\boldsymbol{I_{bat,discharge}}$, $\boldsymbol{I_{branch,discharge}}$) have been calculated in equations (17-20) from the data provided by the cell manufacturer, shown in Table IV.

Table IV. – Parameter values of the storage systems [13], [15].

Battery

Parameter	*Value*	*Description*
V_{cell}	3.7 V	Cell voltage
C_{cell}	21 Ah	Cell capacity
W_{cell}	0.31 kg	Cell weight

Hydrogen tank

Parameter	*Value*	*Description*
$d_{volum,tank}$	9.5 l/kg	Tank volume per kg
P_{tank}	1000 bar	Nominal pressure

$$n_{cells} = \frac{E_{mec\ bat}}{C_{cell} \cdot V_{cell}} \quad (17)$$

$$V_{branch} = n_{series} \cdot V_{cell} \quad (18)$$

$$I_{bat,discharge} = \frac{P_{mec,bat}}{V_{branch}} \quad (19)$$

$$I_{branch,discharge} = \frac{I_{bat,discharge}}{n_{paral}} \quad (20)$$

The weight of the batteries to be installed W_{bat} has been calculated in equation (21) just multiplying the number of cells by the weight of each cell.

$$W_{bat} = n_{cells} \cdot W_{cell} \quad (21)$$

To calculate the total weight of the hydrogen tank to be installed, the weight of the hydrogen $W_{tot,hyd}$ to be contained has been calculated in equation (22), and the volume of this hydrogen at ambient pressure $Vol_{hyd,atm}$ and at nominal pressure of the system $Vol_{hyd,1000}$ in equation (23) and equation (24) respectively.

$$W_{tot,hyd} = W_{flight,hyd} + W_{taxi,hyd} \quad (22)$$

$$Vol_{hyd,atm} = W_{tot,hyd} \cdot Vol_{spec,hyd} \quad (23)$$

$$Vol_{hyd,1000} = Vol_{hyd,atm} \cdot \frac{F_{compr,1000}}{P_{tank}} \quad (24)$$

With this data, the weight of the hydrogen tank $W_{tank,hyd}$ has been calculated in equation (25) and the weight of the water generated as by-product, in equation (26).

$$W_{tank,hyd} = \frac{Vol_{hyd,1000}}{d_{volum,tank}} \quad (25)$$

$$W_{water,fc} = W_{tot,hyd} \cdot \frac{n_{H_20}}{n_{H_2}} \quad (26)$$

Where $\boldsymbol{n_{H_20}}$ and $\boldsymbol{n_{H_2}}$ represent the number of moles of water and hydrogen involved in the reactions.

The energy available at the landing E_{land} which could be recovered by regenerative braking has been calculated in equation (27) from the general kinetic expression.

$$E_{land} = \frac{1}{2} \cdot m \cdot v_{land}^2 \quad (27)$$

This energy can be recovered with a wide range of power outputs which are dependent on the time used to stop completely the jet, and directly proportional to the desired braking distance.

To choose an optimum braking distance x_{max}, an emergency state has been considered based on the following assumptions:

- Reverse thrust in engines and disc brakes in wheels are disabled.
- Aerodynamical devices such as flaps are disabled.

Furthermore, to obtain the maximum safety braking distance, coefficients *A* and *B* are calculated in equations (27) and equation (28), respectively.

$$A = g \cdot \left(\frac{T_0}{W} - \mu\right) \quad (27)$$

$$B = \frac{g}{W} \cdot \left[\frac{1}{2} \cdot \rho \cdot S \cdot (C_D - \mu \cdot C_L) + \alpha\right] \quad (28)$$

where g is the gravity [m/s^2], T_0 is the thrust [N], W is the maximum landing weight [N], μ is the rolling coefficient in the wheels, ρ is the mean density of the air [kg/m^3], S is the wings surface [m^2], C_D is the drag coefficient, C_L is the lift coefficient and $\boldsymbol{\alpha}$ is the relation between the actual thrust and the thrust when the wind speed is null, which corresponds to zero when landing.

Equation (29) shows the calculation of the maximum safety braking distance $\mathrm{x_{max}}$ [m] taking into account the aerodynamic parameters of the jet and the friction of the wheels with the ground.

$$x_{max} = \frac{1}{2 \cdot B} \cdot \ln\left(\frac{A - B \cdot v_{land}^2}{A}\right) \quad (29)$$

The obtained safety braking distance is 2,098.9 m. Knowing the previously calculated energy available at landing, the global coefficient of friction μ_{syst} can be obtained as shown in equation (30).

$$\mu_{syst} = \frac{E_C}{m \cdot g \cdot x_{max}} \quad (30)$$

This way, the term calculated in equation (30) not only represents the coefficient of friction between the wheels and the ground but also represents the friction between the jet and the air. Kinematic laws expressed in equations (31) and (32) are used to calculate the new values of acceleration a and braking time t depending on braking distance x.

$$x = x_0 + v_{land} \cdot t + \frac{1}{2} \cdot a \cdot t^2 \quad (31)$$

$$v = v_{land} + a \cdot t \quad (32)$$

Braking is disabled when the speed v decreases to 10.29 m/s, which is the taxiing speed at which the airliner moves along the runway. Finally, power P necessary to stop the airplane is obtained in equation (33).

$$P = \frac{E_C - \mu_{sist} \cdot m \cdot g \cdot x_{max}}{t} \quad (33)$$

The change in the weight of the airliner $W_{total,plus}$ has been calculated by adding the weight of the new equipment W_{added} and subtracting the weight corresponding to the substituting elements W_{saved} as shown in equations (34)-(36).

$$W_{total,plus} = W_{added} - W_{saved} \quad (34)$$

$$W_{added} = W_{flight,hyd} + W_{taxi,hyd} + W_{bat} + W_{fc} + W_{tank,hyd} \quad (35)$$

$$W_{saved} = W_{tire,sav} + W_{flight,ker} + W_{taxi,ker} + W_{rec,ker} + W_{water} \quad (36)$$

where $W_{flight,hyd}$ is the hydrogen weight necessary in flying, $W_{taxi,hyd}$ is the weight of the hydrogen necessary for taxiing, W_{bat} is the weight of the batteries, W_{fc} is the weight of the fuel cell, $W_{tank,hyd}$ is the weight of the hydrogen tank, W_{convs} is the weight of the converters, $W_{tire,sav}$ is the weight saved in wheels, $W_{flight,ker}$ is the weight of kerosene for flying, $W_{taxi,ker}$ is the weight of kerosene for taxiing, $W_{rec,ker}$ is the weight of kerosene not needed due to the energy recovered and W_{water} is the weight of the necessary water.

Grouping terms in relation to kerosene the weight variation is got and expressed in equation (37) and equation (38).

$$W_{ker,sav,flight} = W_{flight,ker} + W_{taxi,ker} + W_{rec,ker} \quad (37)$$

$$W_{ker,sav,year} = W_{ker,sav,flight} \cdot 365 \frac{flights}{year} \quad (38)$$

4. Simulation Results and Discussion

It is decided that the regenerative brakes come into operation when the plane has moved along 500 meters on the runway, as this prevents generated current peaks from being extremely high. These peaks could cause great problems of excessive heating in the batteries and the coils of the generators.

In Figure 2 the total power of the regenerative braking system to be installed is shown according to the desired braking distance.

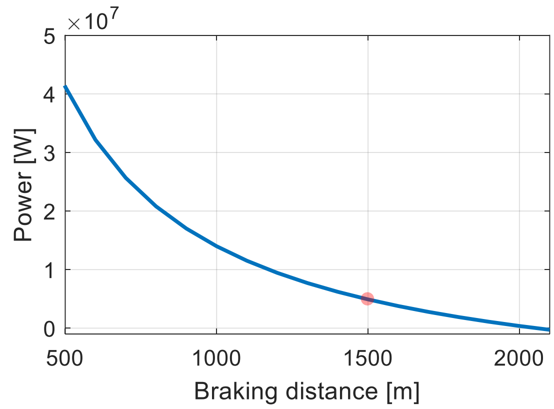

Fig. 2. Power available in regenerating braking across the braking distance.

A braking distance of 1,500 m has been chosen which corresponds to 36.36 s braking time. Thus, an average braking power of 4.91 MW and a deceleration of 1.70 m /s^2 has been obtained.

In Figure 3 the payback is shown in years depending on the hydrogen price. It can be seen that hydrogen prices below 1.7 €/kg offer paybacks of less than 20 years.

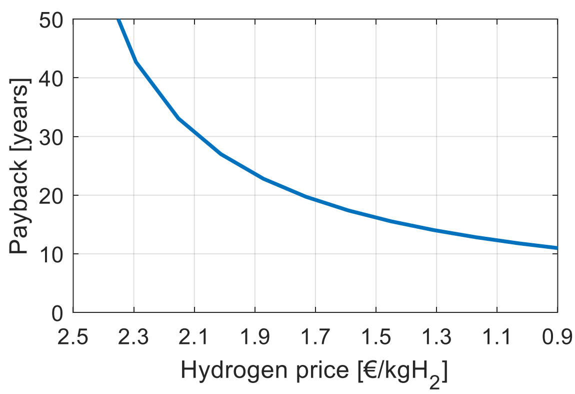

Fig. 3. Payback graph across different Hydrogen prices.

Hydrogen cost obtained by electrolysis is estimated to be 1.93 €/kg approximately in 2020 [16], resulting in a payback of the proposed system of 24 years.

It has been demonstrated that there is an enormous amount of energy that is currently wasted, since it is not used to generate any work, becoming heat due to friction in the mechanical braking system. In the proposed system, the energy recovered and stored during the landing is used in the next flight for taxiing, so that it is possible to reduce in part the necessary energy to be supplied to the battery before starting a new flight.

Regarding the weight variation, the weights of all the additional elements have been added, such as fuel cells, hydrogen tank, wheels and battery motors; also, the assumed weight of the converters. Similarly, the weight of water generated by the fuel cells as by-product has been removed, since it is an amount of water no longer required to be carried in the aircraft in the time of take-off because of being generated on flight. The weight of the removed tires is also subtracted, and the weight of the kerosene equivalent to the energy generated by the proposed systems; This includes kerosene used for traction saved in taxiing before take-off and after landing, the used for on-board power generation during the flight and the saved by energy regeneration during landing.

Fuel savings are directly dependent on the price that Hydrogen can adopt in the coming years.

5. Conclusions

This paper has presented an optimal micro grid to supply the electrical consumptions of a commercial long-distance jet airliner, recover energy during landing and propel the airliner during taxiing movements. The micro-grid is composed of two PEMFCs, power converters, a hydrogen tank, li-ion cells and a set of in-wheel reversible synchronous machines.

The optimal design proposed has allowed reducing the amount of water needed at the time of landing because it is obtained from the by-product of the electrochemical reactions of fuel cells during the flight. Besides, it has allowed a reduction of 370 tons/year in CO_2 emissions due to a reduction in kerosene consumption. Economically, considering a reasonable price of hydrogen (1.7 €/kg) there would be a net savage of 14,070 €/year per airliner in terms of fuel with a null alteration of the total weight of the airplane.

Although the analysis for optimal location of all the equipment has not been realised, it will be developed in future work. This aspect could allow to optimise the energy fluxes and reduce the total energy needed. All other relevant factors have been taken into account in the analysis, although several assumptions have been made due to the lack of information about the costs of the non-commercial equipment used, the price of labour for the installation, the pilot's decisions regarding the landing, weather conditions and many other factors.

Taking into account DOE's forecasts regarding hydrogen production costs for 2020, if a central production system were used, the payback would be about 19 years, which makes the proposed microgrid configuration attractive from the economic and environmental point of view.

References

[1] BP Statistical Review of World Energy. Full report. 66th edition, June 2017.

[2] Eurostat. Final energy consumption by sector. [Last accessed: 20/10/17]. Available online in: http://ec.europa.eu/eurostat/web/products-datasets/-/tsdpc320

[3] Salvi BL, Subramanian KA, Panwar NL. Alternative fuels for transportation vehicles: a technical review. Renew Sustain Energy Rev 2013;25:404e19.

[4] Hari TK, Yaakob Z, Binitha NN. Aviation biofuel from renewable resources: routes, opportunities and challenges. Renew Sustain Energy Rev 2015;42: 1234e44.

[5] Siemens Corporative webpage. Available on line in: http://www.industry.siemens.com/drives/aan/es/electric-motor/pages/default.aspx [Last accessed: 30/11/2017]

[6] M. Brain, "How Lithium-ion Batteries Work", How Stuff Works. Available on line in: http://electronics.howstuffworks.com/everyday-tech/lithium-ion-battery.htm. [Last accessed: 24/11/2017].

[7] PowerTech Systems, "The Lithium Difference". Available on line in: https://www.powertechsystems.eu/home/tech-corner/lithium-ion-battery-advantages/[Last accessed: 24/11/2017].

[8] R. Riazor, J. Rafecas and A. Sudrià, "Ultracondensadores: mayor densidad de energía". Automática e Instrumentación, n. 405, pp. pág. 50-53, 2009.

[9] F. Barreras and A. Lozano, "Hidrógeno. Pilas de combustible de tipo PEM" LITEC, CSIC – University of Zaragoza, 2012.

[10] Hydrogenics, "Fuel Cells". Available on line in: http://www.hydrogenics.com/technology-resources/hydrogen-technology/fuel-cells/[Last accessed: 23/11/2017].

[11] DOE Hydrogen Program, "Hydrogen Fuel Cells". October 2006. Available on line in: https://www.hydrogen.energy.gov/pdfs/doe_fuelcell_factsheet.pdf [Last accessed: 02/12/2017].

[12] Ballard Corporative webpage. Available in: http://www.ballard.com/ [Last accessed: 30/11/2017]

[13] Amicell Corporative webpage. Available in: http://www.amicell.co.il/batteries/ [Last accessed: 30/11/2017]

[14] Boeing Commercial Airplanes, "747-400. Airplane Characteristics for Airport Planning". 2002.

[15] Composite Technology Development Corporative webpage. Available in: http://www.ctd-materials.com/ [Last accessed: 30/11/2017]

[16] DOE "Technical Targets for Hydrogen Production from Electrolysis". Available on line in: https://energy.gov/eere/fuelcells/doe-technical-targets-hydrogen-production-electrolysis [Last accessed 27/12/2017]